Simulation of Decay of Shielding Currents in ITER-TF Joint Samples*)

Shinsaku IMAGAWA[1,2)], Hideki KAJITANI[3)], Tetsuhiro OBANA[1,2)], Suguru TAKADA[1,2)], Shinji HAMAGUCHI[1,2)], Hirotaka CHIKARAISHI[1)], Yuta ONODERA[1)], Kazuya TAKAHATA[1,2)], Kunihiro MATSUI[3)] and Norikiyo KOIZUMI[3)]

[1)]*National Institute for Fusion Science, NINS, Toki 509-5292, Japan*
[2)]*The Graduate University for Advanced Studies, SOKENDAI, Toki 509-5292, Japan*
[3)]*Fusion Energy Directorate, National Institutes for Quantum Science and Technology, Naka 311-0193, Japan*

(Received 18 December 2021 / Accepted 17 February 2022)

As a qualification test of ITER-TF coils, each joint sample was tested prior to manufacture of each TF coil. Eleven joint samples were tested by a conductor test facility with a 9 T split coil. The joint sample comprised two short TF conductors that had twin-box joint terminals at both ends. The lower joint is a testing part that is a full-size joint of the TF coil. Hall probes were attached on the lower joint box to measure the field induced by shielding currents. In order to simulate the shielding currents, an equivalent current circuit has been considered. The main loop of the shielding currents is the current flow in two conductors with crossing the jointed plane twice. The other two loops are the current loops inside superconducting cables in the two conductors. The resistance of the latter loops is given by twice the value of an average contact resistance between the superconducting strands. The calculated results are in good accordance with the experimental data, with an assumption that the overall joint resistance is decreased at low current. This phenomenon can be explained by the existence of a few strands contacting the joint box with extremely low joint resistances.

Keywords: cable-in-conduit conductor, contact resistance, current dependence, joint resistance, Nb_3Sn, shielding current, sintering, twin-box joint

DOI: 10.1585/pfr.17.2405021

1. Introduction

A Nb_3Sn cable-in-conduit (CIC) conductor is adopted for Toroidal Field (TF) coils of ITER. One of the TF coils consists of seven double-pancake coils that are jointed to the neighbor coils at the lower position with "twin-box" joints [1, 2]. In order to attain low joint resistance in nΩ, the Nb_3Sn strands are directly jointed to a copper sleeve of the box by sintering, and the copper sleeve is jointed to that of the adjacent box by soldering [3, 4]. The resistance of the ITER-TF coil joints is required to be less than 3 nΩ at 2 T of background field.

Each joint sample was tested prior to manufacture of each TF coil. Eleven joint samples including two trial samples were tested by a conductor test facility, which was equipped with a 9 T split coil and a dc 75 kA power supply at National Institute for Fusion Science [5, 6]. The joint sample comprised two short TF conductors that had twin-box joint terminals at both ends. The lower joint is a testing part that is a full-size joint of the TF coil. Hall probes were attached on the lower joint to clarify the amount and decay time constant of shielding currents, which were utilized for estimation of AC losses [7]. The magnetic field induced by shielding currents in the joints can be estimated from the difference between the measured magnetic field strength and the magnetic field generated by the external field coil (9 T split coil).

In order to simulate the shielding currents in ITER-TF joint samples, an equivalent current circuit for the shielding currents has been considered. The main loop of the shielding currents is the current flow in two conductors with crossing the jointed plane twice. The other two loops are the current loops inside the superconducting cables in the left-leg conductor and the right-leg conductor. Calculated results for shut-off of the external field coil are in good accordance with the experimental data with the assumption that the overall joint resistance is decreased to one-fourth to one-half at low total current. This paper intends to summarize the simulation method and results and to discuss the current dependence of the overall joint resistance.

2. Experimental Set Up and Results

An ITER-TF conductor consists of a multi-stage twisted cable, a center channel, and a conduit [4]. The cable consists of 900 Nb_3Sn strands and 522 copper strands. A joint sample consists of two short TF conductors with a length of 1,535 mm. The lower joint is a testing part that

author's e-mail: imagawa@nifs.ac.jp

*) This article is based on the presentation at the 30th International Toki Conference on Plasma and Fusion Research (ITC30).

is a full-size joint of the TF coil, where the strands contact the copper sleeve of the joint box by a length of 440 mm, as shown in Fig. 1. A straight section of a length of 300 mm is prepared for voltage taps to measure the voltage drop in the lower joint. In the joint box, the cable is compacted from a void fraction of 33% to 25%. The cable and the copper sleeve are tightly contacted by sintering through heat treatment of the sample for production of the A15 phase of Nb_3Sn. The copper sleeves of the lower joint are jointed to each other with PbSn solder.

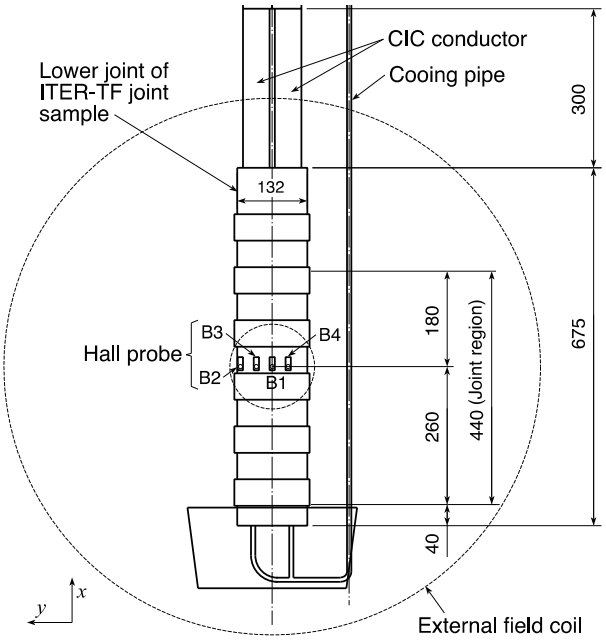

Fig. 1 Setup of an ITER-TF joint sample in the 9 T test facility. B1 to B4 show positions of Hall probes. B1 is located near the center of the external field coil.

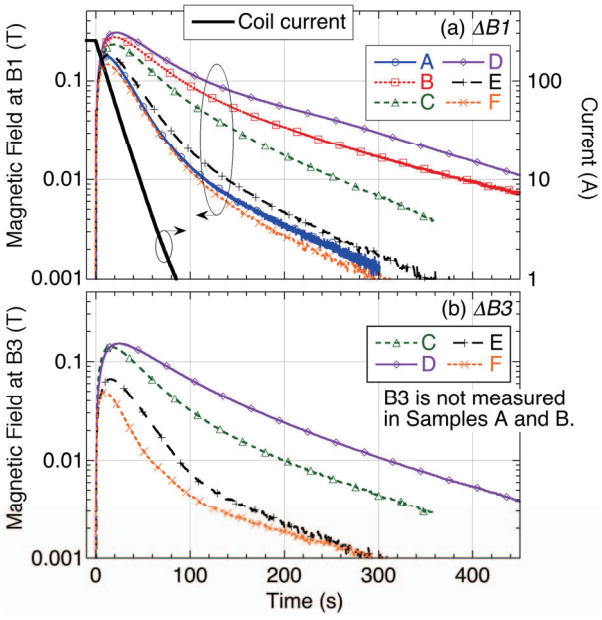

Fig. 2 Measured magnetic field at B1 (a) and B3 (b) positions by shielding currents in the joint samples A to F after shut-off of the external field coil from 1.0 T.

Hall probes are attached on the lower joint at the jointed plane of the two conductors (B1), at the edge of one conductor (B2), and at the middle of each conductor (B3 and B4), as shown in Fig. 1. The vertical positions of these four Hall probes are the same as the center of the external field coil. All the Hall probes measure the field parallel to the axis of the external field coil. The magnetic fields induced by shielding currents in the joint were estimated from the difference between the measured magnetic field strength and the magnetic field calculated from the current of the external field coil [7].

Figures 2 (a) and 2 (b) show estimated magnetic fields induced by shielding currents in six joint samples after shut-off of the external field coil from 1.0 T with an external dump resister. ΔB_1 and ΔB_3 are the fields at the B1 and B3 positions, respectively. The time constant of current decay of the external field coil is 14.7 s. ΔB_1 is higher than ΔB_3, and the decay time constants of the shielding currents are gradually elongated with decrease of the shielding currents for all joint samples.

3. Simulation Model

We have considered three major current loops, as shown in Fig. 3. One is the main current loop, Loop1, where the shielding current flows in two conductors with crossing the jointed plane twice. The other two loops, Loop2 and Loop3, are coupling currents in the left-leg and

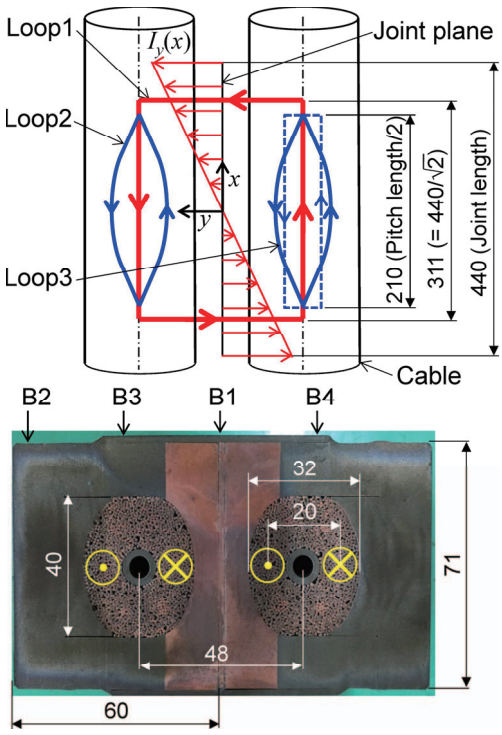

Fig. 3 Cross-section of the joint and a sketch of top view of major loops of shielding currents.

right-leg conductors. ΔB_1 is affected mainly by Loop1, and ΔB_3 is affected mainly by Loop1 and Loop2. Equations of the electric circuits are given by

$$L_0 \cdot dI_0/dt + M_{01} \cdot dI_1/dt + 2M_{02} \cdot dI_2/dt = -R_0 \cdot I_0, \quad (1)$$

$$M_{01} \cdot dI_0/dt + L_1 \cdot dI_1/dt + 2M_{12} \cdot dI_2/dt = -R_1 \cdot I_1, \quad (2)$$

$$M_{02} \cdot dI_0/dt + M_{12} \cdot dI_1/dt + L_2 \cdot dI_2/dt = -R_2 \cdot I_2, \quad (3)$$

where L, M, R, I, and t are the self inductance, mutual inductance, resistance, current, and time. The suffixes 0, 1, and 2 mean the external field coil, Loop1, and Loop2, respectively. The parameters of Loop3 are the same as Loop2, and their mutual inductance is ignored. From the specification of the external field coil, $L_0 = 2.5$ H and $R_0 = 0.17\,\Omega$. Then the decay time constant, $\tau = 14.7$ s.

In the case of uniform joint resistance, the density of current crossing the jointed plane is proportional to the induced voltage in the CIC conductors. Since the voltage is proportional to the interlinkage flux induced by the external field coil, the crossing current per unit length, $I_y(x)$, is approximately given by $2I_1 x/x_0^2$ where x is the distance from the center of the joint, and $2x_0$ is the joint length (see Fig. 3). Therefore, the vertical length of current center of Loop1 is given by $2x_0/\sqrt{2} = 0.331$ m. Joule heating by $I_y(x)$ is given by $R_j/(2x_0) \int I_y(x)^2 dx = 16R_j{I_1}^2/3$ where R_j is the overall joint resistance of the lower joint. Thus, R_1 is given by $4R_j \times 4/3$. L_1 is estimated at 0.112 μH as two parallel conductors with a length of 0.311 m, a diameter of 32 mm, and 48 mm.

The current loops in a superconducting cable in a CIC conductor can be represented by one loop that is formed by the final (5th) stage sub-cables because its decay time constant should be the longest among the current loops in the cable. L_2 is estimated at 0.084 μH as two parallel conductors with a length of 0.21 m (one-half of the twist pitch of the 5th stage), a diameter of 6 mm, and a distance of 20 mm. R_2 is given by twice the value of the average contact resistance between the Nb_3Sn strands, which is reported to be in the range of 1 - 30 nΩ [8–11]. The electric parameter of Loop3 is assumed to be the same as Loop2. Since the mutual inductance can be estimated from the interlinkage flux, $M_{01} = 56.8$ μH, $M_{02} = 10.9$ μH, and $M_{12} = 0.0112$ μH.

Calculated results with constant R_1 and R_2 for Sample D are shown in Figs. 4 (a) to 4 (c). Although the calculated field within 50 s is in good accordance with the experiment, the behavior of both ΔB_1 and ΔB_3 after 50 s is not accorded with the experiment for any R_2. Therefore, the shielding current in Loop2 should be decreased faster than that in Loop1, and the decay time constant of the shielding current in Loop1 should be decreased at low current.

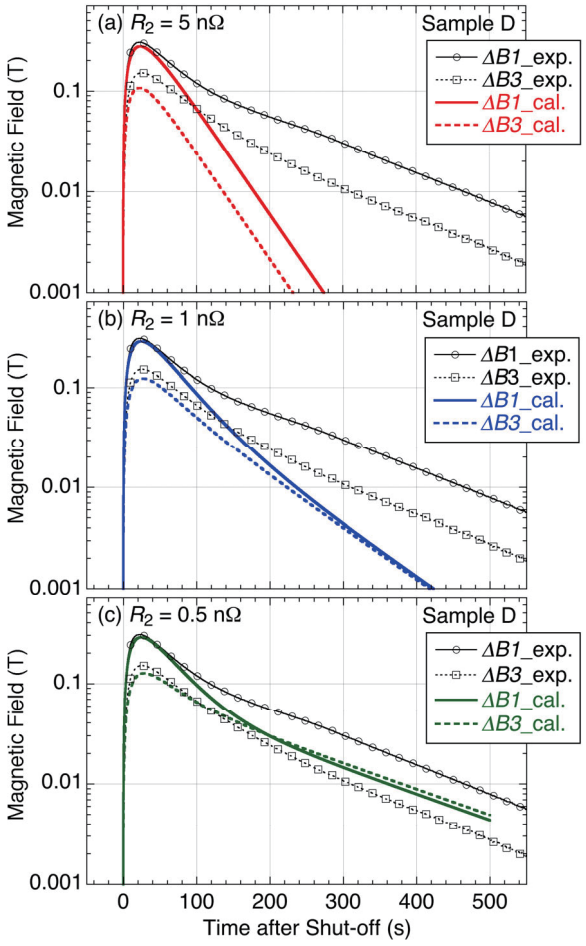

Fig. 4 Magnetic field by shielding currents of Sample D. Thick lines show filed calculated with constant R_1, and the markers show experimental data.

4. Current Dependence of Joint Resistance

Since each strand is jointed to the copper sleeve with individual joint resistance, $R_S(i)$, the current of each strand, $I_S(i)$, is given by $V/R_S(i)$ but less than I_c where V is the average voltage drop in the lower joint, and I_c is the critical current. At first, we assume that the voltage distribution in the copper sleeve is negligibly small in the longitudinal direction. The overall joint resistance of the conductor, R_j, is given by $V/\sum I_S(i)$ that is written as $1/\sum(\mathrm{Min}(1/R_S(i), I_c/V))$.

Next, we assume that $R_S(i)$ obeys normal distribution with the standard deviation of one third of the average value, and that the lowest $R_S(i)$ is 1/500 of the average value. In the case of R_j of 1.0 nΩ and the number of strands of 900, the average joint resistance of each strand is 900 nΩ, and 1/500 of the average is 1.8 nΩ, a half of which corresponds to a good contact with a length of 0.05 m of a strand to the copper sleeve. The calculated R_j for various sets of low $R_S(i)$ is shown in Fig. 5 in the case of I_c of 2.0 kA. The overall joint resistance, $R_j(I)$, can be well fitted by

$$R_j(I)/R_{j0} = \mathrm{Max}(C_0,\ 1 - \alpha/(I + \alpha)), \quad (4)$$

where R_{j0} is the overall joint resistance estimated from the increase rate at high current, and C_0 is the ratio of the lowest overall resistance to R_{j0}. α is a fitting parameter that is related to I_c and the number of strands reaching I_c.

5. Calculated Results and Discussion

The voltage drops in the lower joint of ITER-TF joint samples were measured under several background fields at 1 kA, 15 kA, 30 kA, 45 kA, 60 kA, and 68 kA while holding the current for 300 s to eliminate the effect of shielding currents. Since the joint resistance of the lower joint is estimated from the incline of the linear regression line for the data at 15 kA, 30 kA, 45 kA, 60 kA, and 68 kA, this resistance is treated as R_{j0} in the following calculation. The dependence of R_{j0} on the magnetic field is shown in Fig. 6 for Samples A to F. The linear regressions of $R_{j0}(B)$ are given by

$$R_{j0}(B) = 0.518 + 0.091B \text{ [n}\Omega\text{] for Sample D,} \quad (5)$$

$$R_{j0}(B) = 1.475 + 0.154B \text{ [n}\Omega\text{] for Sample E,} \quad (6)$$

$$R_{j0}(B) = 1.843 + 0.148B \text{ [n}\Omega\text{] for Sample F,} \quad (7)$$

where B [T] is the magnetic field at the coil center.

Using equations (1) to (7), calculated results for Sample D is shown in Figs. 7 (a) and 7 (b), and for Samples E and F in Figs. 8 (a) and 8 (b), respectively. R_2, α, and C_0 are fitting parameters. The calculated results are in good accordance with the experiment with the parameters in Table 1. Since α is estimated at 6 - 12, a few strands should be jointed to the copper sleeve with low resistance

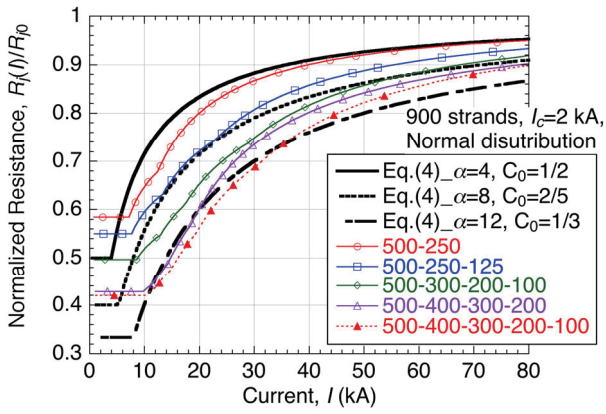

Fig. 5 Calculated overall joint resistance in cases with very low individual joint resistances of strands. The number such as 500 - 250 means that the individual joint resistances are 1/500 and 1/250 of the average.

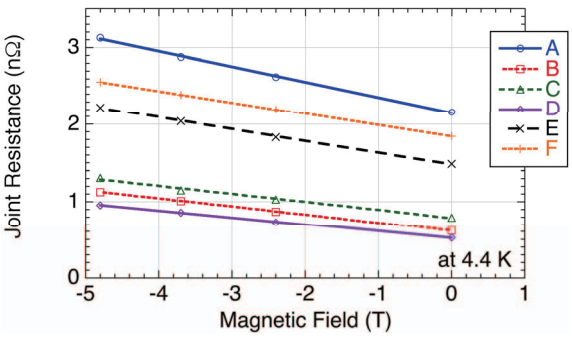

Fig. 6 Dependence of joint resistances on the magnetic field.

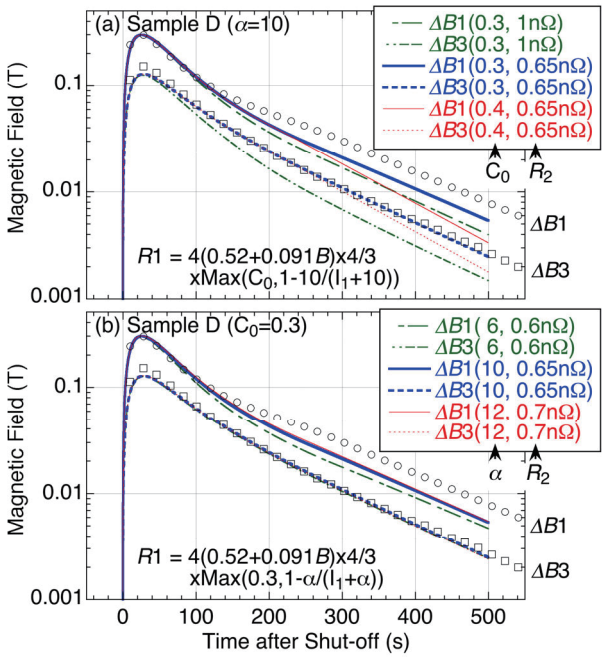

Fig. 7 Calculated magnetic field by shielding currents of Sample D for α = 10 (a) and C_0 = 0.3 (b). The markers show experimental data.

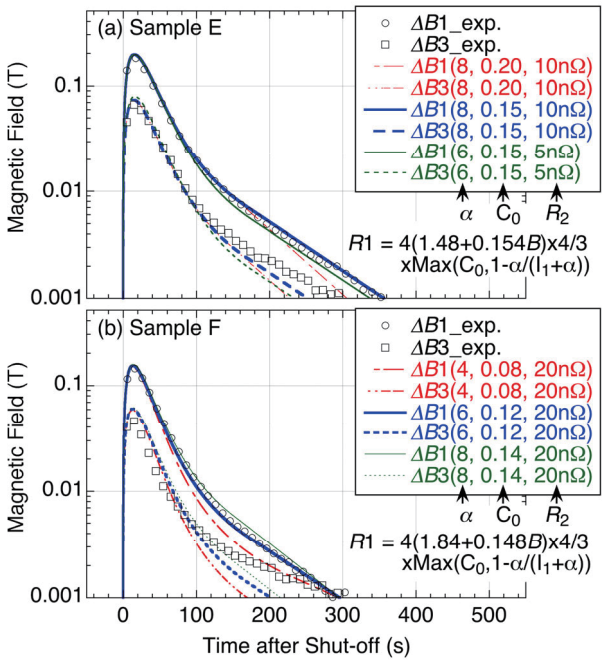

Fig. 8 Calculated magnetic field by shielding currents of Sample E (a) and Sample F (b). The markers show experimental data.

Table 1 The best values of fitting parameters for calculation of shielding currents in Samples D, E, and F.

Sample	α	Co R_{j0} (nΩ)	R_2 (nΩ)
D	10-12	0.16	0.65-0.7
E	8	0.22	10
F	6	0.24	10-20

in the order of 1 nΩ, and their currents should reach I_c. Since the lowest overall joint resistance is around 0.2 nΩ in all the three samples, the lowest joint resistance between each strand and the copper sleeve should be around 1 nΩ, even in Samples E and F, the overall joint resistances of which are relatively high. The contact resistance between strands of Sample D is estimated at around 1 nΩ, and those of Samples E and F are 10 - 20 nΩ. These values are consistent with the references [8–11].

As shown in Fig. 2, the apparent decay time constant of Sample D around 200 s is slightly longer than that after 300 s. This phenomenon can be explained by a shift of current center with the shielding currents decreasing. In the case that a strand with very low joint resistance is located at a position close to B1, the current center of Loop1 is shifted to the B1 position at low current.

The very long, more than 600 s, decay time constant of ΔB_3 after 200 s in Samples E and F cannot be simulated with the three current loops. This field should be induced by minor current loops that are formed by a few strands tightly contacting each other for long length.

6. Summary

The magnetic field induced by shielding currents in an ITER-TF joint sample can be simulated with three current loops. The main loop is the current flow in two conductors with crossing the jointed plane twice. The other two loops are current loops inside superconducting cables in the two conductors. The calculated results for shut-off of the external field coil are in good accordance with the experiment with three assumptions. (1) Overall joint resistance of a CIC conductor is decreased at low current and can be fitted by $1-\alpha/(I+\alpha)$ where I and α are the current and fitting parameter related to the critical current and the number of strands reaching the critical current. (2) The lowest overall joint resistance is around 0.2 nΩ. (3) Contact resistance between strands is 1 - 20 nΩ.

The current dependence of the overall joint resistance can be explained by considering the existence of a few strands contacting the copper sleeve of the joint box with low joint resistances in the order of 1 nΩ.

∗The views and opinions expressed herein do not necessarily reflect those of the ITER Organization.

Acknowledgment

This work was performed with contracted research with JAEA, collaborative research with Mitsubishi Electric Corp., collaborative research with Toshiba Corp., and the NIFS Collaboration Research program (NIFS10 ULAA003, NIFS12KECA017, NIFS17KECA051).

[1] C. Sborchia, Y. Fu, R. Gallix, C. Jong, J. Knaster and N. Mitchell, IEEE Trans. Appl. Supercond. **18**, 463 (2008).
[2] P. Decool, D. Ciazynski, A. Nobili, S. Parodi, P. Pesenti, A. Bourquard and F. Beaudet, Fusion Eng. Des. **58-59**, 123 (2001).
[3] B. Stepanov, P. Bruzzone, S. March and K. Sedlak, Fusion Eng. Des. **98-99**, 1158 (2015).
[4] H. Kajitani, T. Hemmi, T. Mizutani, K. Matsui, M. Yamane, T. Obana, S. Takada, S. Hamaguchi, K. Takahata, S. Imagawa and N. Koizumi, IEEE Trans. Appl. Supercond. **25**, 4202204 (2015).
[5] S. Imagawa, H. Kajitani, T. Obana, S. Takada, S. Hamaguchi, H. Chikaraishi, K. Takahata, K. Matsui, T. Hemmi and N. Koizumi, IEEE Trans. Appl. Supercond. **28**, 4200405 (2018).
[6] H. Kajitani, S. Imagawa, T. Obana, S. Takada, S. Hamaguchi, H. Chikaraishi, M. Nakamoto, M. Yamane, K. Yoshizawa, Y. Uno, K. Matsui, N. Koizumi and M. Nakahira, IEEE Trans. Appl. Supercond. **31**, 9369847 (2021).
[7] S. Imagawa, H. Kajitani, T. Obana, S. Takada, S. Hamaguchi, H. Chikaraishi, Y. Onodera, K. Takahata, K. Matsui and N. Koizumi, IOP Conference Series **1857**, 012013 (2021).
[8] N. Koizumi, Y. Takahashi, Y. Nunoya, K. Matsui, T. Ando, H. Tsuji, K. Okuno, K. Azuma, A. Fuchs, P. Bruzzone and G. Vecsey, Cryogenics **42**, 675 (2002).
[9] F. Cau and P. Bruzzone, Supercond. Sci. Technol. **22**, 045012 (2009).
[10] F. Bellina, M. Breschi and P.L. Ribani, IEEE Trans. Appl. Supercond. **20**, 482 (2010).
[11] P. Bruzzone, B. Stepanov, R. Dettwiler and F. Staehli, IEEE Trans. Appl. Supercond. **17**, 1378 (2007).